Space weather capabilities of low frequency radio arrays

Joseph E. Salah[•a], Colin J. Lonsdale[a], Divya Oberoi[a], Roger J. Cappallo, Justin C. Kasper[b]
[a]MIT Haystack Observatory, Westford, MA, USA 01886-1299
[b]MIT Center for Space Research, Cambridge, MA, USA 02139-4307

ABSTRACT

Radio arrays currently operating below 1 GHz have observed interplanetary scintillations of radio sources to derive valuable information on the density and velocity of the solar wind and coronal mass ejections. New large radio arrays are currently in the design and development phase, and are characterized by wide fields of view, high sensitivity, and multiple beam capabilities. One such array, the Mileura Widefield Array – Low Frequency Demonstrator (MWA-LFD) in Western Australia (26.4°S, 117.3°E), is being designed for operation at 80 to 300 MHz. Its characteristics include a 15-50° field-of-view, 16 simultaneous beams, and an effective collecting area of 8000 m^2 at 200 MHz with 32 MHz instantaneous bandwidth resulting in a point-source sensitivity of 20 mJy for an integration time of one second. The array consists of 8000 dual-polarization dipoles, clustered in sub-arrays that are spread over a 1.5 km diameter and connected to a central digital signal processor. The MWA-LFD will participate in the global network of observatories that monitor solar bursts and interplanetary scintillations, and will improve the spatial and time resolution of solar wind characterization by increasing both the number of radio sources that can be used for scintillation measurements and the number of observations that can be made in a given time period. In addition, the MWA-LFD will be able to provide observations of the Faraday rotation of polarized radio sources, thus allowing the possibility of determining the evolution of the magnetic field in a coronal mass ejection. The design of the array, the signals expected to be received by the array, and the requirements and challenges for the space weather observations are discussed in this paper.

Keywords: Space weather, solar wind, heliosphere, coronal mass ejections, radio arrays, low frequency.

1. INTRODUCTION

Key observations needed for improving our understanding of the heliosphere and space weather include the density, velocity, and magnetic field in the solar wind particularly during solar disturbances. Remote sensing via radio techniques can be applied to determine such parameters, and allows coverage of the vast heliosphere from close to the solar surface to the Earth so that the evolution of these parameters can be tracked. Of particular importance for space weather is the measurement of the magnetic field of a coronal mass ejection (CME) which governs the degree of coupling of CME energy to the terrestrial magnetosphere, thus allowing a prediction of the impact of the solar storm on Earth.

Radio remote sensing techniques have been successfully applied for heliospheric studies primarily through the measurement of the interplanetary scintillations of radio sources using single or multiple stations to determine plasma density and speed[1,2,3,4]. Radio tomography has also been used to map three-dimensional views of the solar wind[5,6,7,8]. Other remote sensing techniques have utilized radio tracking of spacecraft that occulted the corona to determine magnetic fields through Faraday rotation[9,10] and one such study has identified a CME[11]. Recently, several radio galaxies were observed with the VLA and used to study the structure of the heliospheric current sheet[12], and a CME was imaged through direct imaging at radio wavelengths[13].

With the advent of a new generation of large radio arrays, particularly those planned to operate at low frequencies, the capabilities of remote sensing methods to study the heliosphere will be greatly enhanced[14,15,16]. Such large arrays provide higher sensitivities and resolution than previously available, and remove some of the constraints imposed by the sparse spatial and temporal sampling of the heliosphere provided by current instruments.

• jsalah@haystack.mit.edu; phone 1 781 981-5400; fax 1 781 981-0590; haystack.mit.edu

Solar Physics and Space Weather Instrumentation, edited by Proceedings of SPIE Vol. OEI133 (SPIE, Bellingham, WA, 2005) · 0277-786X/05/$15 · doi: 10.1117/12.613448

This paper describes the design of a new array, called the Mileura Widefield Array - Low Frequency Demonstrator (MWA-LFD). The array will consist of 500 stations operating at frequencies in the range 80 – 300 MHz, and will be located at a radio-quiet region in Western Australia. The project, a collaborative effort between US and Australian institutions and researchers, will provide measurements on solar bursts, heliospheric structure, and CME magnetic fields that will advance knowledge of the heliosphere and space weather.

2. DESCRIPTION OF THE ARRAY

The important characteristics of a radio array for heliospheric research are: (a) sensitivity so that a large number of radio sources can be observed, (b) wide field-of-view so that a large area of the heliosphere can simultaneously be covered, and (c) angular resolution so that the location of solar bursts can be determined precisely. The operational frequency of a radio array is one of the factors that govern these parameters as well as the magnitude of the plasma effects that we seek to measure. The radio propagation effects must be large enough to be observable in as large a part of the heliosphere as possible. For the MWA-LFD, the selected frequency range is 80 – 300 MHz, and has been driven in part by the heliospheric requirements as well as by consideration of other scientific goals for the array such as the detection and imaging of the epoch of reionization in the early universe.

Other notable characteristics of the MWA-LFD design are that the array contains no moving parts since the antenna elements are fixed dipoles, and that it will be pointed by electronic steering. System architecture will be heavily dependent on modern digital processing techniques and software control. Table 1 summarizes the specifications of the MWA-LFD.

Table 1. Array specifications

Frequency Range	80-300 MHz
Number of receptors	8000 dual polarization dipoles
Number of tiles (4x4 dipoles)	500
Effective collecting area[§]	~8000 m^2
Field of view	15°-50°
Configuration	Centrally-condensed pseudo-random array ~1.5 km diameter
Angular resolution[§]	3.4 arcmin
Instantaneous bandwidth	220 MHz (sampled); 32 MHz (processed)
Point source sensitivity[¶]	20 mJy in 1sec; 0.33 mJy in 1 hr
Number of baselines	124,750
Multi-beam capability	Up to 16, per polarization
Width of spectral channel	8 kHz
Number of spectral channels	4000
Time resolution	0.5 sec (imaging), 125 μsec (beamformer)
Polarization	Full Stokes

[§] At 200 MHz [¶] 32 MHz bandwidth at 200 MHz

The MWA-LFD will be an imaging interferometer array consisting of 500 antenna 'tiles', each a 4×4 array of crossed vertical bowtie dipoles, for a total of 8000 dipoles. The tiles will be installed in a region of ~1.5 km diameter, totaling ~8000 m^2 of collecting area at 150 MHz, and produce an electronically-steerable beam with a field-of-view ranging from 15° (at 300 MHz) to 50° (at 80 MHz). Figure 1 shows the planned layout of the array. The basic unit is the antenna tile which is connected to an analog beamformer producing RF on coax. Tiles are assembled into nodes which are scattered within the array. In order to optimize the point spread function, the nodes are scattered across the ~1.5 km aperture, with a degree of central condensation. There will be 64 nodes of 8 tiles each.

The entire 80-300 MHz RF from each tile is digitized at the corresponding node, decimated to a selected 32 MHz subset of the full range of the array, spectrally filtered to 4K channels of 8 kHz resolution, and transported to a central processing facility. These channels are fed to a large digital correlator. Overall, 125,000 baselines are correlated, producing ~4 billion visibilities every half second. These visibilities are used by to produce calibrated snapshot images of the full 15-50 degree field-of-view every half-second in 4K frequency channels. The input to the correlator is also shared with a digital beamformer for tracking of a limited number of sources with high temporal resolution.

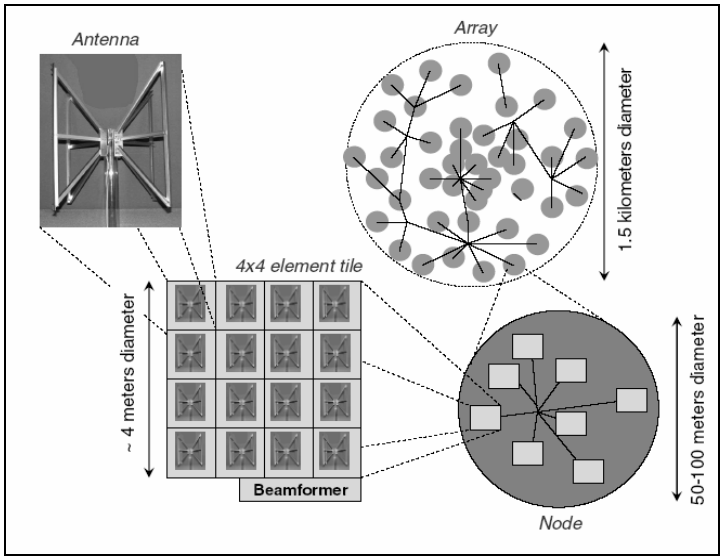

Figure 1. Schematic of the physical layout of the array.

Each of the main components of the MWA-LFD is described briefly below.

2.1 Antenna tiles

The prototype MWA-LFD element is a pair of crossed, bowtie antennas of open-frame construction that will be installed over a ground screen. The arms are broad enough to provide the impedance match with the low noise amplifier (LNA) over the wide frequency range of 80 to 300 MHz, and they have been made symmetric about the horizontal to reduce the E-plane antenna gain near the horizon at the higher frequencies. The open construction affords low wind resistance and light weight, thereby simplifying the mechanical support. Figure 2 shows the prototype dipole antenna, manufactured by Seavey, Inc., with the active balun in the inset, and presents the simulated and measured antenna patterns.

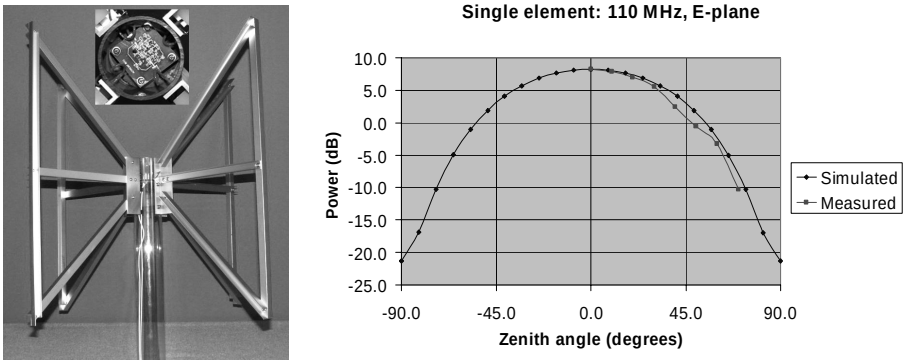

Figure 2. Prototype MWA dipole and antenna pattern

An open-wire-mesh screen measuring ~6x6-m will form the ground plane for the tile, as shown in Figure 3, together with the 16 dipoles that form a tile. An analog beamformer for each tile, with electronic steering capability, will be located at the edge of the ground plane to minimize the loss in the RF cables from the LNAs. In each beamformer chassis will be two boards, one per polarization, with coplanar waveguide delay lines for 16 antennas and a 16-way combiner on each board, as well as the digital electronics to control them. A prototype beamformer used for initial testing of the antenna tile is also shown in Figure 3. The two polarization output signals will be amplified sufficiently to overcome the loss in the cables between the beamformer and the receiver, which may be a few tens of meters away. Measured antenna gain patterns for the tile showed a 40^{o} beam-width at 140 MHz, as specified.

Figure 3. A 16-dipole antenna tile and beamformer used in tests at Haystack Observatory.

2.2 Receivers

The weak RFI environment at the Mileura site in Western Australia allows the use of a direct sampling receiver. The receiver system is defined here to be all components between the RF output of the analog antenna tile beamformer, and a high spectral resolution (8 kHz) digital data stream transmitted to the central processing facility. The receiver consists of two parts. The front end is a small analog & mixed-signal board consisting of a single fixed low-pass and sky-noise equalization filter, final amplifier, and fast A/D converter sampling RF in the first Nyquist zone. The back end is a purely digital part implementing coarse spectral filtering, decimation to a selected 32 MHz subset, final spectral filtering to 4K channels of 8 kHz resolution, and aggregation of signals for transport via fiber to the central processor.

2.3 Central Processor

The central processor system can be divided into three distinct operations: routing and reordering, cross-correlation, and signal combination. These three functions can be implemented on at most two distinct board designs, with specific functionality depending on the programming of Xilinx FPGAs. The top level architecture of the correlation and digital beamforming system is illustrated in figure 4.

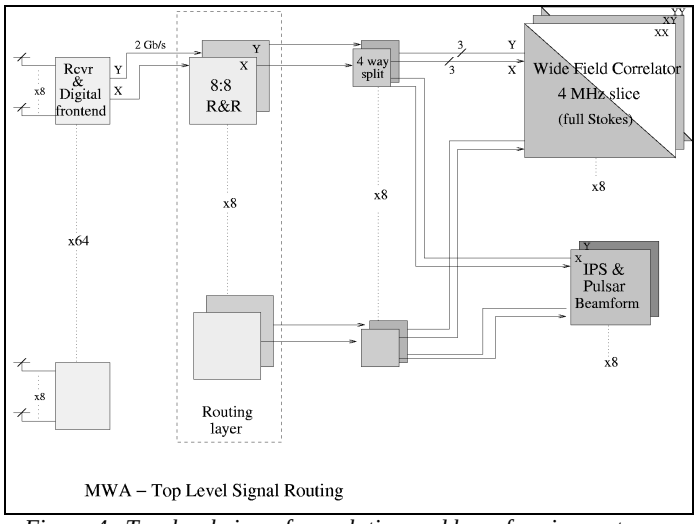

Figure 4. Top-level view of correlation and beamforming systems.

The data coming from the digital receivers will be aggregated into 2 Gb/s serial data streams. Each stream will consist of single-polarization data from 8 antenna tiles, organized as 4K point Fourier transforms of the input samples, and concatenated for each of 8 antennas, repeated at 125 μsec intervals. In order to make efficient use of correlator resources, data streams need to be formed containing more antennas over a smaller band of frequencies. This operation is accomplished within a routing network, the primary component of which is the Routing & Reordering module which is FPGA-based. The routing layer aggregates the data into streams of 64 antennas, and reorders the data (corner turner) to provide suitable input signals for the Wide Field Correlator (WFC).

The correlation module will carry out the cross-multiplication and integration of up to 125,000 antenna pairs for each of 4 polarization products. In order to efficiently utilize the processing power of the FPGAs, the correlator is divided into eight 4 MHz slices to cover the full 32 MHz bandwidth. The cross-correlations are formatted and dumped at 0.5 s intervals in order to maintain a full field-of-view. The array digital beam-former combines signals from all 500 antennas, which must be brought together at a single location. To accomplish this, hardware similar to the routing layer is fed by one of 4 replicated data streams from the routing layer. Sufficient resources will exist to implement 16 simultaneous beams. The digital beamformer will linearly combine data from all 500 antennas pre-multiplied by appropriate complex phase factors, detect power, and integrate over a time and frequency range appropriate to the application.

2.4 Full Field Imager

The Full Field Imager (FFI) is responsible for calibrating both the instrument and the ionosphere in near real time, producing calibrated snapshot images of the full 15-50 degree field-of-view and generating calibration data suitable for use in the analysis of the scientific data. The ionospheric irregularity length scale is typically much larger than the size of the array, but smaller than the antenna field of view at ionospheric heights. Thus, in any given direction, all baselines encounter the same ionospheric phase gradient, and the apparent sky formed by simple inversion of visibilities will be coherent with source positions distorted in rubber-sheet fashion. Comparison of apparent and actual source positions then yields full ionospheric calibration information. The calibration data will be used to remove the visibility contributions of bright point sources, and contaminating sources from outside the primary field-of-view, in order to eliminate sidelobe confusion capable of interfering with scientific uses of the data. The ionospheric, power pattern, and polarization calibrations are then used to create calibrated images as a function of frequency and polarization.

2.5 Data transport and system monitoring

The digital front-ends will generate an aggregate data rate of 256 Gb/s, which needs to be transported over distances of up to 2 km to the central building for correlation and array beamforming. This can be accomplished simply and economically with off-the-shelf consumer grade components such as transceivers and fiber-optic cables which will terminate at the routing layer. Since the routing is point-to-point, no addressing of packets is needed, and a simple serial format can be utilized to maintain framing. Relatively modest monitor and control software will be needed. The principal control elements are scheduling, antenna tile pointing, frequency selection and excision, and general configuration. The status of each subsystem also needs to be monitored and will be done via a low-bandwidth duplex link to each digital front-end.

2.6 Data products

The principal data products of the array include the raw correlations generated by the WFC, the calibration solutions and snapshot full-field images from the FFI, and the beamformed data from the digital beamformer. The raw correlations are used to accumulate data for statistical analysis and will be stored only briefly. Calibration solutions generated by the FFI include ionospheric parameters as well as antenna power patterns and position-independent gains which will be saved for analysis. The snapshot-calibrated full-field images generated by the FFI will be used by the Faraday Rotation analysis software for heliospheric and space weather observations. The beamformed data streams will be used for the interplanetary scintillation analysis and for any other high time resolution application.

3. SPACE WEATHER APPLICATIONS OF THE MWA-LFD

In this section, we describe briefly the projected applications of the MWA-LFD for heliospheric and space weather studies. Three topics are discussed, namely interplanetary scintillations, Faraday rotation, and solar radio burst imaging.

3.1 Interplanetary Scintillations (IPS)

The IPS technique provides a line-of-sight integral of density irregularities in the outflowing heliospheric plasma by observing short-timescale intensity fluctuations in compact background radio sources. The technique has been employed for many years to derive the density structure and velocity in the heliosphere. The analysis relies upon plasma motions relative to the Earth due to solar rotation and radial motion of the solar wind in order to obtain a range of perspectives and perform tomographic inversion, and some assumptions are made about the propagation and evolution of the plasma structures. This work has been successfully pursued for heliospheric and space weather by several groups[4,6,7,8]. The primary limitation of some of the work, particularly in tomography, has been the sparseness of the spatial and temporal sampling of the heliosphere afforded by the current instruments since sufficient independent measurements are needed to fully constrain the solutions.

The IPS system in the MWA-LFD will be based upon the digital beamformer which is capable of combining the data streams from all 500 antennas to produce many independent, high-quality beams within the antenna's wide field-of-view. The current design will support 16 independent beams. The output of the beamformer will be a time and frequency-averaged time series for every beam, with ~10 msec time resolution, and less than 1 MHz frequency resolution. At 200 MHz, the MWA-LFD will provide a sensitivity of 20 mJy for a 1-second integration in 32 MHz of bandwidth. When combined with the ability to observe many scintillating sources simultaneously, the MWA demonstrator will provide a number of independent IPS measurements that is larger by over an order of magnitude than possible with current systems. At the upper frequencies of its operating frequency range, the array should be able to observe the effects of interplanetary scintillations as close as ~40 solar radii where strong scattering begins to occur. In addition to breaking new ground in enhancing the quality and density of IPS observables, the southern hemisphere location of the MWA-LFD will provide complementary coverage of the solar environment to existing facilities in the northern hemisphere. Heliospheric observations with the MWA-LFD are planned to be targeted daytime observing campaigns followed by offline analysis, and the data will be shared and distributed to the broader solar physics community.

3.2 Faraday rotation (FR)

A polarized electromagnetic wave propagating through magnetized plasma experiences Faraday rotation (FR) which is proportional to the integral of the product of the electron number density and the component of the field along the line-of-sight. The amount of rotation of the linear polarization vector is strongly dependent on wavelength, and varies as wavelength squared. FR due to the solar corona has been measured by tracking spacecraft such as Helios with the Deep Space Network at 2.3 GHz[9], and has been used to determine the mean magnetic field in the corona[10] and in a CME[11].

In order to assess the detectability of FR by the MWA-LFD, a simplified calculation was made using the October 2003 CME event and background heliosphere. For the CME simulation, the measured magnetic field at 1 AU was fit with a simple model of a cylindrically-symmetric flux rope that was mapped back towards the Sun and then propagated towards Earth to calculate the amount of rotation. At 150 MHz, a peak rotation of 1000 degrees was computed at roughly 0.5 AU, decreasing to about 100 degrees at 0.7 AU, and to ~10 degrees near 1 AU. The one-sigma accuracy of the MWA-LFD for measuring the FR of a source with 20 mJy polarized flux in the 80-300 MHz band in a 5-minute observation period is estimated to be about 4 degrees, which is sufficient for the detection of the rotation assuming a sufficient number of polarized sources are available as discussed below.

The polarization vector is expected to undergo several rotations during part of the CME trajectory and the ambiguity needs to be resolved. This can be made through observations of the rotation at several frequencies within the 80 to 300 MHz band as a function of time, and then the time series can be used to trace the rotation through its cycles. It is expected that the MWA will be able to monitor sources within ~50 solar radii from the Sun and the FR effect of a flux rope will become visible through measurements of several hundred background sources by the time the CME is half way to Earth. Once the FR measurements are made, an inversion is required to determine the magnetic field component

in the CME since the FR measurements represent an integral of the electron density and magnetic field component along the observing line-of-sight. Measurements along multiple lines-of-sight will be used for such inversion to determine flux rope properties such as helicity, orientation and size, thus providing the important magnetic properties that are useful for predicting the geo-effectiveness of earthward CMEs.

For the background heliosphere, the task is more challenging since the amount of rotation due to the quiescent heliosphere would be much smaller. Taking into account the limits due to depolarization across the measuring frequency band which weakens the signal, and the effects of angular broadening due to scattering which cause loss of correlated flux density, the range of FR in the quiescent heliosphere will vary from ~ 10 to 10^4 degrees in the 80-300 MHz band depending on the distance from the Sun. We expect the MWA-LFD to cover the range from ~5 to 50 solar radii, and provide up to 400,000 constraints per solar rotation thus allowing comparisons with and possible validations of models of coronal structure and solar wind formation.

There are several challenges that could potentially limit the accuracy of the FR measurements of the heliosphere or CMEs. The first is the effect of the Earth's ionosphere which can vary at 300 MHz from ~50 degrees at noon during solar minimum to several hundred degrees at solar maximum. The effect is a factor of 10 larger at the lower frequencies of the MWA-LFD band. This ionospheric component must be carefully removed from the total FR in order to determine the residual rotation due to the heliospheric phenomena. It is expected that ionospheric FR measurements can be made using differential GPS with an accuracy of a few degrees, as was successfully demonstrated at the VLA[17]. Suitably located dual-frequency GPS receivers at the MWA should thus be able to provide the necessary calibration of the ionospheric contribution to FR with sufficient accuracy to resolve the heliospheric component.

A second challenge relates to the number of polarized radio sources and their intensities in the MWA-LFD frequency range. A recent survey of polarization at 340-370 MHz found 13 extragalactic sources in an area less than 35 deg^2, exhibiting typical polarized intensities of ~20 mJy and readily measurable Faraday rotation[18]. In the 200-300 MHz range of the MWA demonstrator, with a field of view in the 200-400 deg^2 range, we can expect to detect over 100 sources in a 5-minute integration period with a single pointing. The situation is less clear for lower frequencies, but if insufficient extragalactic sources are available, it may be possible to use selected regions of the strong polarized galactic background emission, which has small-scale structure imposed upon it by local interstellar Faraday depolarization[18]. One of the primary early tasks for the MWA-LFD is of course to conduct a polarization survey in the southern hemisphere and at the array's frequencies.

We finally note that the FR and IPS data from the array are complementary. Both techniques yield integral measures of plasma properties, with FR being proportional to magnetic field strength times electron density, and IPS representing the radial component of the solar wind velocity and a measure of turbulence in the medium. The turbulence parameter is proportional to the amplitude of density fluctuations which is loosely proportional to the density. Both IPS and FR can be used together to solve independently for the magnetic field and for the electron density distribution, but data from other sources such as STEREO will be very important to obtain a 3-D dynamic view of the heliosphere.

3.3 Solar burst imaging

Solar radio bursts are manifestations of the macroscopic release of energy in CMEs, solar flares and other evolving magnetic structures, and are believed to be caused by shocks and energetic electrons moving through the solar corona into the interplanetary medium. The potential of low frequency arrays to observe solar radio bursts have been most recently reviewed by several authors[14,15,19].

Of particular interest are type II solar bursts which are generally associated with CMEs[20,21,22]. These bursts are observed[23] below 150 MHz and continue down to a few MHz, drift in frequency on the order of ~-0.2 MHz/sec, and typically last for 5 to 15 minutes. Type II bursts have been associated with *fast* CMEs[21,24,25] since theoretically the radiation would come from the shocks produced by the fast moving ejecta. Thus the CME has to be sufficiently fast to be able to drive a shock in the ambient medium[19]. An alternative explanation for type II bursts is that they are caused by sudden heating of the coronal loops during flares. For the few cases where positional information is available for type II bursts, the radio source seems to occur well behind the leading edge of the CME[26,27,28]. Such an emission can be interpreted as being produced either by flare shocks moving through the CME material or as radio emission from the flanks of a CME-driven shock.

The MWA-LFD will image emission from shocks with unprecedented spatial resolution since its angular resolution would localize bursts to ~3 arc minutes. We thus expect that spatially resolved imaging of burst emission with the MWA-LFD at sufficiently high cadence should be able to shed light on a variety of topics such as the relationship between radio bursts and CMEs and the structure of the emission source and radiation propagation[15]. Finally, a unique capability of the MWA-LFD will be its combined observation of a type II burst at its source followed by the development and evolution of the CME as it traverses interplanetary space.

4. PROJECT STATUS

Preliminary design of the MWA-LFD has been largely completed, and prototyping of some of the key elements of the system has been started in order to feed into a final detailed design. The project is a joint effort between various US and Australian institutions, and proposals for funding the construction of the array are currently pending. The best location for the array was determined after careful consideration of several candidate sites in Australia, Europe and the USA, with emphasis on the radio quietness of the various sites and the long term maintenance of such an environment. At the low frequencies of operation of the MWA-LFD, the radio environment can be a major limitation on the performance, complexity and cost of the array. As a result of radio frequency interference measurements and consideration of other technical issues, a remote, unpopulated, superbly-quiet site in Western Australia was deemed to be ideal for the MWA-LFD. The site is located near the Mileura station (26.4^{o}S, 117.3^{o}E), hence the name Mileura Widefield Array to identify the array's location and its important wide field-of-view characteristic.

In order to begin the testing of prototype array components at the Mileura site, a series of early deployment campaigns were undertaken by the US-Australia project partners in the first half of 2005. The initial goals were to test the durability and performance of the dipole antennas and to make more precise measurements of the radio environment using the actual array elements. Figure 5 shows the first antenna test station deployed at Mileura in March 2005, consisting of 16 dual-polarization dipoles on a ground plane, and the analog beamformer powered by a battery-backed solar generator. The signals from the beamformer were transported ~150m via coax cable to an equipment van where they were converted to an 8 MHz IF, digitized, and stored on a PC for spectral analysis. A second antenna station was deployed in April 2005 and a third in June 2005.

Figure 5. The first completed antenna station with beamformer box and battery-backed solar power supply.

Figure 6 demonstrates the remarkably clean RFI environment at Mileura obtained with the MWA-LFD test station. These deep integrations of 30-60 minutes at representative frequencies of 102, 131, 189 and 327 MHz exhibit rms noise more than 30 dB below the galactic background, yet even at this high sensitivity, large tracts of frequency space show no evidence whatsoever of detectable RFI. Further, most of the observed features exhibit low temporal occupancy. This bodes extremely well for future high sensitivity experiments, solar and heliospheric measurements and other scientific projects.

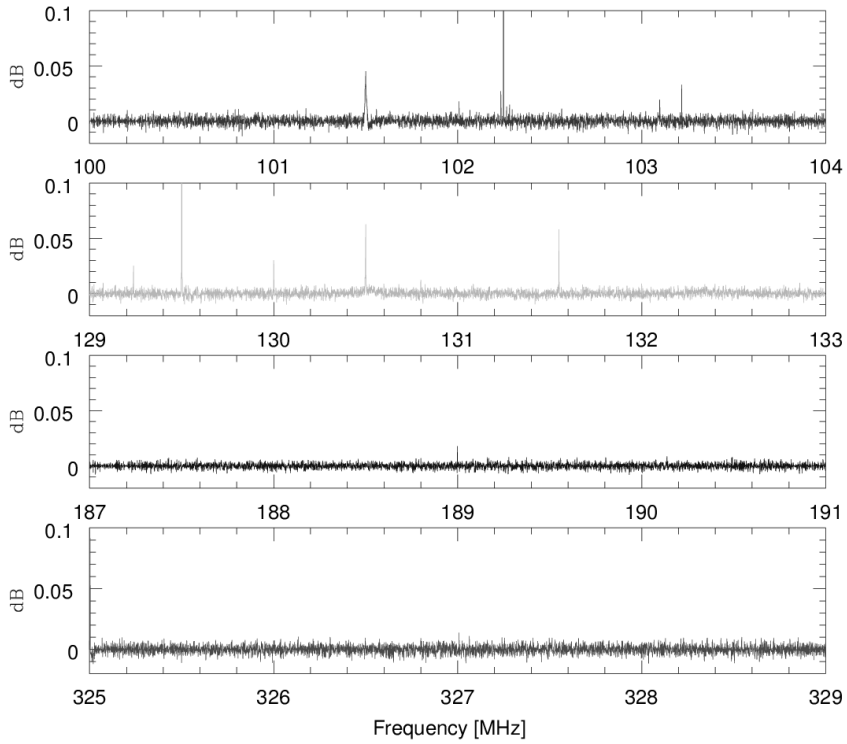

Figure 6. Deep integrations for 4 spectral windows of 4 MHz each, to characterize the low-level RFI environment at Mileura. Integration times at 102, 131, 189 and 327 MHz were 30, 60, 60 and 30 minutes respectively. The scales are in dB relative to the system noise, which is dominated by the sky background. These data have been median-filtered to remove the bandpass shape. Three of the displayed peaks are clipped on these plots; the peak at 102.25 MHz is ~1.5 dB, that at 129.5 MHz is ~1.7 dB, and the one at 325.0 MHz is ~0.16 dB. The resolution bandwidth is 1 kHz.

A drift scan with the station beam pointed at zenith clearly showed transit of the galactic plane at 192 MHz, and demonstrated the sky noise limited performance of the system. Sky maps at various frequencies were then obtained by electronically steering the antenna station beam with the analog beamformer to a set of locations chosen to cover the entire visible sky to 30^o elevation. These tests again showed the transit of the galactic center and the rising of the Sun, and demonstrated the consistency of the images from frame to frame indicating excellent instrumental stability on timescales from seconds to hours.

Interferometry tests between two tiles separated by 145 meters were also carried out, and demonstrated the array's ability to perform precision measurements of a number of discrete unresolved sources on the sky, with accurate fringe rate determinations to isolate contributions from specific sky locations. Several observations were also made of the Sun, with the most extensive being a full interferometry run for 6.5 hours, alternating between 96 and 196 MHz. A series of small flares were recorded as shown in Figure 7. Many short-duration spikes are visible, and the two brightest ones are identified by NOAA monitoring data as low-intensity type-III sweep-frequency radio bursts. There is a smooth phase ramp generated by the changing delay geometry of the observation as the earth rotates. In almost all cases, deviations from this smooth phase ramp are correlated with the spikes. A potential interpretation of this observation is that the solar emission during the spikes has a positional centroid that is displaced from that during quiescent periods.

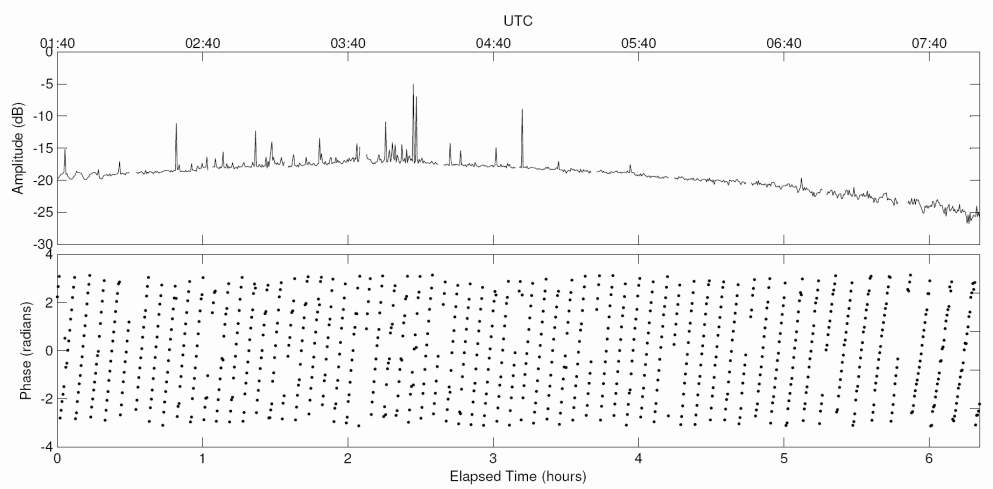

Figure 7. Correlated amplitude and phase at 96 MHz for the Sun over a 6.5 hour period on 27 April 2005. At this frequency and with a baseline of 145 m, one solar diameter corresponds to roughly three radians of interferometer phase.

5. SUMMARY

The MWA-LFD, operating at 80-300 MHz, is characterized by high sensitivity, high resolution, wide field of view, and multiple beams. Its design will allow valuable measurements for solar, heliospheric and space weather studies by applying the techniques of interplanetary scintillations, Faraday rotation, and solar burst imaging. It is projected that construction of the array will occur over a two year period, pending availability of funds. Science operations would nominally start in early 2008.

Partner institutions in the development of the MWA-LFD include MIT's Haystack Observatory and Center for Space Research, the Harvard-Smithsonian Center for Astrophysics, Australia Telescope National Facility, Australian National University, Curtin University of Technology, Melbourne University, and the Office of Science and Innovation in Western Australia. Collaborators in the solar applications include researchers at the University of California San Diego, Bonn University, Nagoya University, and University of Sydney.

ACKNOWLEDGMENTS

Design studies for the array were supported under a grant from the National Science Foundation, Division of Astronomical Sciences, under the Information Technology Research program (AST-0121164). Studies of solar and space weather applications were supported by the NSF Division of Atmospheric Studies under the Solar-Terrestrial Program (ATM-0317957). Further studies are currently underway under an AFOSR grant (FA9550-0510247). We are also grateful to MIT and TruePosition Inc. for support of the construction of the antenna prototypes and the early deployment tests at Mileura.

We also acknowledge various colleagues who were instrumental in the design of the prototype systems and in the testing at Mileura reported in this paper. They include David Barnes, Judd Bowman, Frank Briggs, Brian Corey, David Herne, Eric Kratzenberg, Mervin Lynch, Bruce Stansby, and Jamie Stevens.

REFERENCES

1. Tappin, S. J., Planet. Space Sci., 34, 93-97, 1986
2. Asai, K., Ishida, Y., Kojima, M., Maruyama, K., Misawa, H., and Yoshimi, N., J. Geomag. Geoelectr., 47, 1107-1112, 1995.
3. Manoharan, P.K., Ananthakrishnan, S., M. Dryer, Detman, T. R., Leinbach, H., Kojima, Watanabe, T., and J. Kahn, Solar Phys., *156*, 377, 1995.
4. Fallows, R. A., P. J. S. Williams, A. R. Breen, Ann. Geophys., *20*, 1279, 2002.00
5. Jackson, B. V., Hick, P.L., Kojima, M. and Yokobe, A., Phys. Chem. Earth, 22, 425-434, 1997
6. Jackson, B.V., Hick, P.L., Kojima, M., Yokobe, A., J. Geophys. Res., *103*, 12049, 1998.
7. Kojima, M., Tokumaru, M., Watanabe, H., Yokobe, Asai, K., Jackson, B. V., Hick, P.L., J. Geophys. Res., 1998, *103*, 1981.
8. Tokumaru, M., Kojima, M., Fujikii, K., Yokobe, A., J. Geophys. Res., *105*, 10435, 2000.
9. Bird, M.K. Space Science Review, *33*, 99, 1982.
10. Pätzold, M., Bird, M.K, & Volland, H., Solar Physics, *109*, 91, 1987.
11. Bird, M. K., Volland, H., Howard, R. A., et al., Solar Physics (ISSN 0038-0938), *98*, 341, 1985.
12. Mancuso, S., & Spangler, S.R., Astrophys. J., *539*, 480, 2000.
13. Bastian, T.S., Pick, M., Kerdraon, A., Maia, D., Vourlidas, A., Astrophys Journal, 558:L65-L69, 2001
14. Bastian, T. S., 2004, Planetary and Space Sci., 52, 1381, 2004.
15. Cairns, I. H., Planetary and Space Science, *52*, 1423-1434, 2004.
16. Oberoi, D. and Kasper, J.C., Planetary Space Sci., 52, 1415, 2004.
17. Erickson, W., Perley, R.A., Flatters, C. & Kassim, N.E., Astron. Astrophys., *366*, 1071, 2001.
18. Haverkorn, M., Katgert P., & de Bruyn, A.G., Astron. Astrophys., *403*, 1031, 2003.
19. Gopalswamy, N., Planetary and Space Science, *52*, 1399-1413, 2004.
20. Gopalswamy, N. et al., J. Geophys. Res., *103*, 307-316, 1998.
21. Cliver, E. W., Webb, D. F. and Howard, R. A., Solar Phys. *187*, 89, 1999.
22. Cairns, I. H. and Kaiser, M. L., In Ross Stone, W. (Ed), *Review of Radio Science*, 1999-2002, IEEE Press, 749-774, 2002.
23. Gopalswamy, N., In Stone, R. G., Weiler, K. W., Goldstein, M. L. and Bougeret, J.-L. (Eds), *Radio Astronomy at Long Wavelengths*, Geophysical Monographs, *119*, AGU Press, 123-135, 2000.
24. Gopalswamy, N. et al., Astrophys. J., *486*, 1086, 1997.
25. Gopalswamy, N. et al., Astron. Astrophys., *347*, 684, 1999.
26. Wagner, W. J, and MacQueen, R. M., Astron. Astrophys., *120*, 136, 1983.
27. Gary, D. E. et al., Astron. Astrophys., *134*, 222, 1984.
28. Robinson, R. D. and Stewart, R. T., Solar Phys., *97*, 145, 1985.